Proc. Natl. Acad. Sci. USA
Vol. 78, No. 3, pp. 1346–1350, March 1981
Biochemistry

Mechanism of the actomyosin ATPase: Effect of actin on the ATP hydrolysis step

(muscle/pre-steady-state kinetics/myosin/cross-bridge action)

LEONARD A. STEIN*, P. B. CHOCK†, AND EVAN EISENBERG*

*Laboratory of Cell Biology and †Laboratory of Biochemistry, National Heart, Lung, and Blood Institute, National Institutes of Health, Bethesda, Maryland 20205

Communicated by Terrell L. Hill, September 29, 1980

ABSTRACT **The Lymn–Taylor model for the actomyosin ATPase suggests that during each cycle of ATP hydrolysis the complex of myosin subfragment 1 (S-1) with actin must dissociate into S-1·ATP plus actin before ATP hydrolysis can occur. In the present study we tested whether such a mandatory detachment step occurs by measuring the effect of actin on the rate and magnitude of the ATP hydrolysis step (initial P_i burst) and on the steady-state ATPase rate. We find that the rate of the initial P_i burst markedly increases at high actin concentration although the Lymn–Taylor model predicts the rate should remain nearly constant or decrease. In addition, at high actin concentration, the magnitude of the initial P_i burst is much larger than is predicted by the Lymn–Taylor model. Finally, at 360 μM actin, at which more than 90% of the S-1·ATP is bound to actin, there is no inhibition of the steady-state ATPase activity although the Lymn–Taylor model predicts that 70% inhibition should occur. We conclude that the acto–S-1 complex is not dissociated by ATP during each cycle of ATP hydrolysis; in fact, the rate of the initial P_i burst appears to be even faster when S-1·ATP is bound to actin than when it is dissociated.**

In 1971, on the basis of pre-steady-state kinetic studies using the soluble fragments of myosin, heavy meromyosin and subfragment 1 (S-1), Lymn and Taylor (1) proposed the following kinetic model for the actomyosin ATPase:

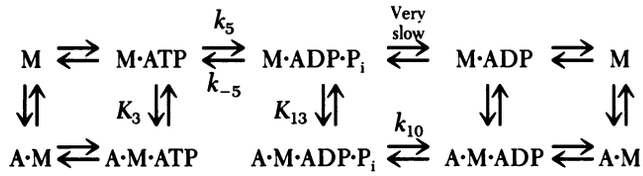

Scheme I

in which A is actin and M is myosin.

The most important feature of this model is the postulate that the actual ATP hydrolysis step, M·ATP → M·ADP·P_i, occurs only when M·ATP is detached from actin. This feature of the model requires myosin to detach from actin during each cycle of ATP hydrolysis, a point that has major implications for the mechanism of cross-bridge action *in vivo* (2). Therefore, it is important to determine whether ATP hydrolysis is indeed prevented when M·ATP is bound to actin, particularly because recent evidence suggests that a detachment step may not always be required when actomyosin hydrolyzes ATP *in vitro* (3, 4).

The most direct method of determining whether the ATPase cycle includes a mandatory detachment step is to study the effect of actin on the ATP hydrolysis step (initial P_i burst) because in the Lymn–Taylor model this step occurs only with the S-1 detached from actin. In the present study we determined the effect of actin on the rate and magnitude of the initial P_i burst. In addition, we determined the effect of very high actin concentration on the steady-state ATPase rate. The results of all of these experiments show that, if anything, the rate of the ATP hydrolysis step is even faster when S-1 is bound to actin than when it is dissociated from actin. This indicates that S-1 is not required to detach from actin during each cycle of ATP hydrolysis.

MATERIALS AND METHODS

Myosin (5), actin (6), and chymotryptic S-1 (7) were prepared as described and their protein concentrations were determined spectrophotometrically (3).

Measurements of the rate of fluorescence enhancement and the turbidity of acto–S-1 solutions were carried out in a stopped-flow apparatus as described (3). Quenched-flow experiments were carried out in a Durram D-132 multimixer, as described (8) except that, to facilitate mixing, the pressure was held constant at 80 psi (552 kilopascals) and the quench time was varied by changing the length of the reaction tubing. To minimize hydrolysis of ATP by F-actin when F-actin was pre-mixed with ATP, the F-actin was incubated with 100 μM nonradioactive ATP for 1 hr prior to addition of 100 μM [γ-^{32}P]ATP and then used within 10 min. The small amount of ATP hydrolysis caused by actin alone was corrected for by running a control in the absence of S-1.

At actin concentrations below 100 μM, steady-state ATPase activity was measured by using the pH-stat (9). At higher actin concentrations, [^{32}P]P_i production was assayed directly. Each run consisted of five time points; the rate was always linear. To avoid the inhibition of the extraction of P_i by high actin concentration, 0.3-ml samples were first quenched with 0.2 ml of 0.8 M KCl/20 mM MgATP and then HCl and silicotungstic acid were added and P_i was extracted as described (8). [γ-^{32}P]ATP (New England Nuclear) was standardized as described (8).

THEORY

This section presents analytic expressions for the steady-state ATPase rate and the rate and magnitude of the initial P_i burst as predicted by the Lymn–Taylor model (scheme *I*). The derivation of these equations will be presented elsewhere.

We assume that a rapid equilibrium exists between M·ATP and A·M·ATP and between M·ADP·P_i and A·M·ADP·P_i and also

The publication costs of this article were defrayed in part by page charge payment. This article must therefore be hereby marked "*advertisement*" in accordance with 18 U. S. C. §1734 solely to indicate this fact.

Abbreviations: S-1, subfragment 1 of myosin; A, actin; M, myosin.

that $K_3 = K_{13}$. On this basis, the rate of the initial P_i burst predicted by the Lymn–Taylor model is:

$$k_{obs} = \frac{(k_5 + k_{-5})K_3 + k_{10}[A]}{(K_3 + [A])}. \quad [1]$$

Note that, at high actin concentration, k_{obs} approaches k_{10}.

We define the magnitude of the P_i burst as

$$P^{burst}_{i(t)} \equiv P^{measured}_{i(t)} - M_{total}\,Vt \quad [2]$$

in which t is time after the S-1, ATP, and actin are mixed in the quenched flow apparatus, $P^{measured}_{i(t)}$ is the total P_i present after acid quench at time t; M_{total} is the concentration of added S-1; and V is the steady-state ATPase rate. Thus, the P_i burst is defined as the extra P_i produced over and above the P_i that would theoretically be present if steady-state conditions prevailed from $t = 0$. Note that, in general, the value of $P^{burst}_{i(t)}$ is less than the actual amount of M·ADP·P_i + A·M·ADP·P_i present at time t because in reality there will be a lag in the development of the steady-state ATPase rate. On this basis, for the Lymn–Taylor model,

$$V = \frac{k_{10}k_5K_3[A]}{[(k_5 + k_{-5})K_3 + k_{10}[A]]\,[K_3 + [A]]} \quad [3]$$

$$P^{burst}_{i(t)} = \frac{M_{total}\,k_5(k_5 + k_{-5})K_3^2}{[(k_5 + k_{-5})K_3 + [A]]^2}(1 - e^{-k_{obs}t}). \quad [4]$$

Note that at high actin concentration $P^{burst}_{i(t)}$ approaches 0.

In the model of Stein *et al.* (3), similar (although more complex) equations were used to compute k_{obs}, $P^{burst}_{i(t)}$, and V.

RESULTS

To test whether the Lymn–Taylor model, with its mandatory detachment step, can account for the steady-state and presteady-state kinetic behavior of the actomyosin ATPase, numerical values must be obtained for the rate constants and equilibrium constants in this model under a specific experimental condition. The data obtained by stopped-flow turbidity measurements (15°C; $\mu = 0.13$ M) for the steady-state binding of S-1 to actin in the presence of ATP can be fitted by a simple hyperbolic plot with an equilibrium constant of $3 \times 10^4\ M^{-1}$ (Fig. 1*a*) When S-1 was mixed with actin and ATP under these conditions, the steady-state level of binding was attained within the dead-time of the stopped-flow apparatus (Fig. 1*a Inset*) and did not change during the time course of the initial P_i burst (first 50–100 msec of the reaction as shown in Fig. 2*a*). Therefore, in agreement with previous data (3), M·ATP and M·ADP·P_i are in rapid equilibrium with A·M·ATP and A·M·ADP·P_i, respectively, and, under the conditions of Fig. 1, the equilibrium constants K_3 and K_{13} have a value of $3 \times 10^4\ M^{-1}$.

The sum of k_5 and k_{-5}, the forward and reverse rate constants of the initial P_i burst in the absence of actin, was determined by using two different methods. First, the time course of P_i production was measured directly by using rapid acid quench (Fig. 2*a*). Second, the rate of fluorescence enhancement, which has been shown to be mainly due to the initial P_i burst (10, 11), was measured by using stopped flow. The two measurements were generally in good agreement; the rate constant for P_i production was 19 sec^{-1} and the rate constant for fluorescence enhancement was 23 sec^{-1}. In previous studies, the rate constant for P_i production was also found to be about 20% lower than the rate constant for fluorescence enhancement (10, 11). Because the efficiency of mixing is better in the two-syringe apparatus than in the three-syringe apparatus, we have assumed in the present study that $k_5 + k_{-5} = 23$ sec^{-1}. (The assumption that $k_5 + k_{-5} = 19$ sec^{-1} would not have significantly affected the conclusions presented in this paper.)

$K_5 = k_5/k_{-5}$ can be determined by comparing the magnitude of the initial P_i burst (M·ADP·P_i) with the magnitude of the irreversibly bound ATP (M·ATP + M·ADP·P_i). The latter value was obtained by mixing S-1 with [γ-^{32}P]ATP and then rapidly quenching with a large excess of unlabeled ATP. If all of the S-1 were fully active, the magnitude of the irreversibly bound ATP would be 1 mol/mol of added S-1. We found that, with chymotryptic S-1, the magnitude of the irreversibly bound ATP was generally about 0.8 mol/mol of added S-1—i.e., about 80% of the S-1 is active. Because we found that the magnitude of the initial P_i burst is 0.6 mol/mol of added S-1 (Fig. 2*a*), $K_5 = 3$ and therefore $k_5 \simeq 17$ sec^{-1} and $k_{-5} \simeq 6$ sec^{-1}, in agreement with previous measurements (3, 9–11).

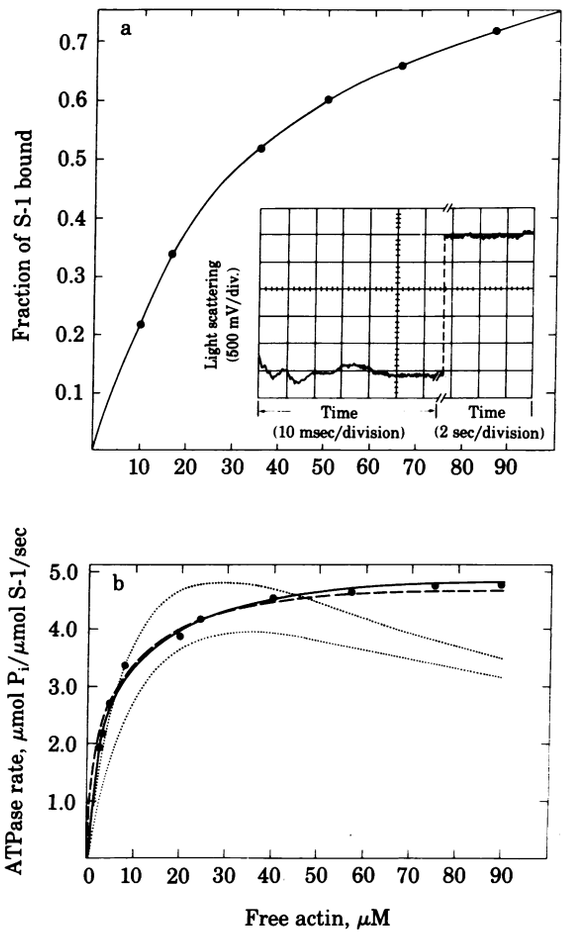

FIG. 1. (*a*) Fraction of S-1 bound to actin in the presence of ATP. Conditions: 10 mM imidazole, 1.8 mM $MgCl_2$, 1 mM ATP, 10–30 μM S-1, pH 7.0, 15°C. ●, Experimental data determined from stopped-flow turbidity measurements; solid line, theoretical binding curve for $K = 3 \times 10^4\ M^{-1}$. (*Inset*), Time course of development of turbidity. Actin + ATP in one syringe was mixed with S-1 in the second syringe in the stopped-flow apparatus. The flow stopped at the beginning of the trace. Conditions were the same as above with 33 μM actin and 20 μM S-1. Note that the mixing artifact seen early in the trace is small compared to the total turbidity change. (*b*) Actin-activated S-1 ATPase activity. Conditions were the same as in (*a*) except 3 mM imidazole and 1 μM S-1 were used. ●, Experimental data; solid line, best fit to experimental data with $K_{app} = 5.5 \times 10^{-6}$ M; dotted lines, predictions of Lymn–Taylor model with $k_{10} = 20$ (lower curve) or 30 (upper curve) sec^{-1}; dashed line, prediction of Stein *et al.* model.

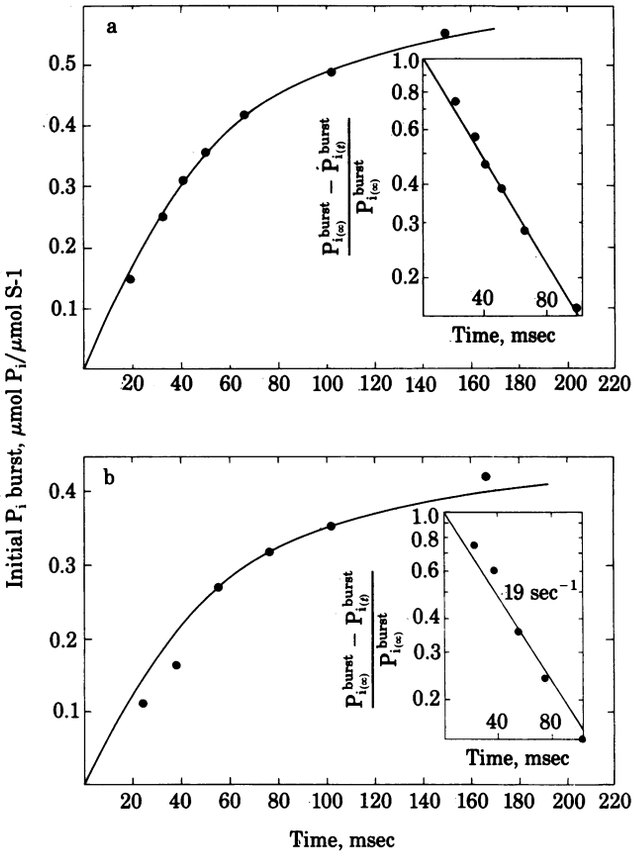

FIG. 2. Time course of the initial P_i burst in the absence of actin (*a*) and with 8 μM actin (*b*). Conditions as in Fig. 1 except 100 μM ATP and 20 μM S-1 were used. (*Insets*) First-order plots of the data. Solid lines in the direct plots and insets yield a rate constant of 19 sec^{-1} for both *a* and *b*.

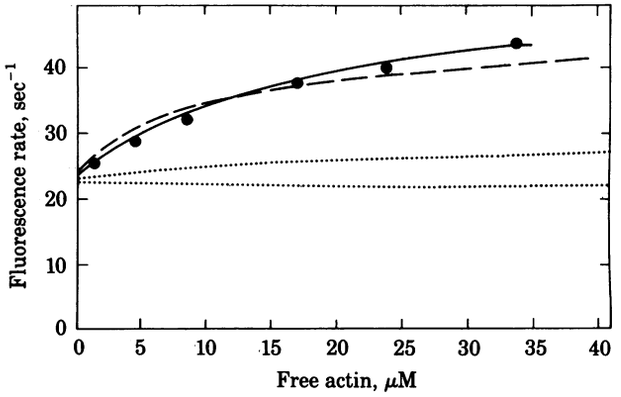

FIG. 3. Rate of fluorescence enhancement as a function of actin concentration. Conditions as in Fig. 1*a*. ●, Experimental data; solid line, best fit to experimental data; dotted lines, predictions of Lymn–Taylor model with k_{10} = 20 (lower curve) or 30 (upper curve) sec^{-1}; dashed line, prediction of Stein *et al.* model.

Because we are working at saturating ATP concentration, the only other rate constant needed to test the Lymn–Taylor model is k_{10}. The range of possible values for k_{10} was determined by fitting the acto–S-1 ATPase activity at varying actin concentrations by using Eq. 3 and the values of K_3, K_{13}, k_5, and k_{-5} determined above. The solid line in Fig. 1*b* shows a typical plot of ATPase activity versus actin concentration; the upper and lower dotted lines show the plots predicted by Scheme I with k_{10} = 20 sec^{-1} and 30 sec^{-1}, respectively. Clearly, for Scheme I to account for these data, k_{10} must have a value between 20 and 30 sec^{-1}. This agrees reasonably well with the value of 15 sec^{-1} which we assumed for k_{10} in our previous experiments (3) in which the acto–S-1 ATPase activity was about 20% lower than in our present experiments.

Rate of the Initial P_i burst. We can now test if the Lymn–Taylor model is able to account for the kinetic behavior of the actomyosin ATPase. The effect of actin on the rate of the initial P_i burst was determined by measuring the rate of fluorescence enhancement at varying actin concentrations. The rate constant increased from 23 sec^{-1} in the absence of actin to 45 sec^{-1} at 40 μM actin (Fig. 3). It is not possible to perform this experiment at higher actin concentrations because the fluorescence of the actin itself begins to interfere with the accuracy of the measurement. Nevertheless, it is clear that the rate of the initial P_i burst increased as the actin concentration increased. In contrast, the Lymn–Taylor model predicts (dotted lines in Fig. 3) that the apparent rate constant of the initial P_i burst (k_{obs}, Eq. 1) should either decrease (k_{10} = 20 sec^{-1}) or remain nearly constant (k_{10} = 30 sec^{-1}) as the actin concentration increases. This is because, in the Lymn–Taylor model at high actin concentration, the equilibrium between A·M·ATP and M·ATP is shifted toward A·M·ATP which decreases the overall rate of the transition from M·ATP to M·ADP·P_i and makes the rate constant of the initial P_i burst approach k_{10} (Eq. 1).

It is difficult to see how the rate constant of the initial P_i burst could nearly double at high actin concentrations unless the initial P_i burst occurred without dissociation of the acto–S-1 complex. Indeed, these data suggest that the P_i burst may be even faster when S-1·ATP is bound to actin than when it is dissociated from actin (see *Discussion*).

Magnitude of the Initial P_i Burst. We could not determine the magnitude of the initial P_i burst from fluorescence data because the turbidity of the acto–S-1 complex, as well as the fluorescence of the actin itself, might interfere with this measurement. Therefore, we measured the magnitude of the initial P_i burst by directly assaying P_i production with the three-syringe quenched-flow apparatus. The most important difference between the measurements of the initial P_i burst in the presence and absence of actin is the correction that must be made for the high steady-state ATPase rate in the presence of actin. In each of our experiments, the steady-state ATPase activity was measured at the same time as the pre-steady-state P_i release by using the three-syringe quenched-flow apparatus with long delay times. The initial P_i burst was defined as the excess P_i produced above the value expected if the steady-state ATPase were linear from time zero (see Theory).

Fig. 2*b* shows the time course of the initial P_i burst at 8 μM actin; at this concentration, actin should have relatively little effect on the rate and magnitude of the initial P_i burst but the steady-state ATPase rate was quite high. Therefore, this experiment served as a control for experiments at higher actin concentration. Comparison of Fig. 2*b* with Fig. 2*a* shows that the time course and magnitude of the initial P_i burst at 8 μM actin are similar to what we observed in the absence of actin; the magnitude was decreased about 30% (see below for discussion of this point) and the rate constant was nearly the same. Based on the fluorescence data in Fig. 4, the rate constant might be expected to be slightly higher. However, mixing is not as efficient in the three-syringe apparatus as in the specially designed cell of the two-syringe apparatus. Therefore, an increased rate may be masked to some extent by mixing occurring in the delay line of the three-syringe apparatus.

We next measured the magnitude of the initial P_i burst at 70

μM actin. The Lymn–Taylor model predicts that the magnitude of the initial P_i burst should decrease to a low level at this actin concentration (Fig. 4) and at even higher actin concentration should approach 0 (Eq. 4). This is because, in the Lymn–Taylor model, the overall rate of formation of A·M·ADP·P_i from A·M·ATP is greatly decreased at high actin concentration but the rate of product release (k_{10}), and hence the rate of re-formation of A·M·ATP, is quite rapid. The solid symbols in Fig. 4 show that, in contrast to this prediction, the magnitude of the initial P_i burst is significant at 70 μM actin. To make certain that this result was valid and not due to a mixing artifact, we mixed the actin and ATP in two different ways: actin + ATP in the first syringe and S-1 in the second syringe (● in Fig. 4), and acto–S-1 in the first syringe and actin + ATP in the second syringe ($\times_r$ and ▲ in Fig. 4). This second method of mixing ensured that the S-1·ATP was always exposed to a high actin concentration. The results were the same with both methods of mixing. However, when we attempted to mix all of the acto–S-1 in the first syringe with ATP in the second syringe, the time course of P_i release became somewhat slower (data not shown). Undoubtedly, this is because of the high viscosity of the acto–S-1 complex in this experiment.

Even when the S-1 and actin + ATP were kept in separate syringes, the 140 μM actin solution was quite viscous. Therefore, no attempt was made to determine an apparent rate constant from the data in Fig. 4; at the very high actin concentration used in this experiment, the mixing itself probably took 10–20 msec to complete as the viscous solutions flowed through the delay line of the three-syringe apparatus. This probably explains why the rate of P_i release in this experiment was considerably slower than what would be expected on the basis of the fluorescence experiments (Fig. 3), which showed that actin increased the rate of the initial P_i burst. Because the correction for the steady-state ATPase rate is applied from time zero, relatively slow mixing will also decrease the observed magnitude of the initial P_i burst to a small extent. Nevertheless, the data in Fig. 4 show that at high actin concentration the magnitude

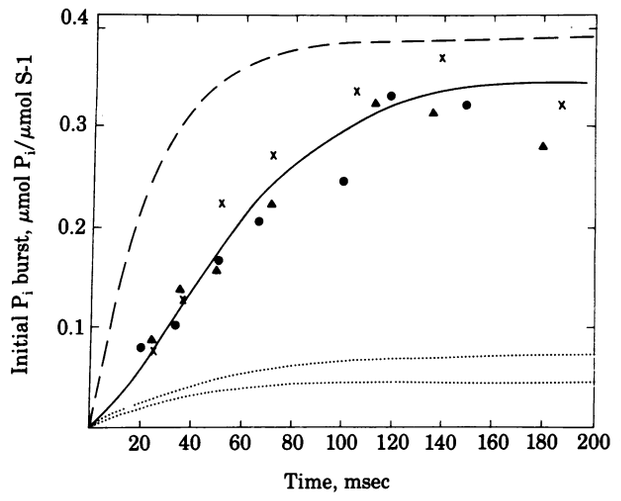

FIG. 4. Magnitude of the initial P_i burst at 72 μM actin; conditions as in Fig. 2*b*. ●, S-1 in first syringe (final concentration, 20 μM) mixed with actin + ATP in second syringe (third syringe contained 2 M HCl); ▲, ×, actin + S-1 in first syringe mixed with actin + ATP in second syringe. For each experiment the steady-state ATPase rate was independently determined with 1-sec delay times in the three-syringe apparatus (rate constants = 4.0–5.0 sec^{-1}) and extra P_i produced above the steady-state production was calculated as described under *Theory*. Dotted lines, prediction of Lymn–Taylor model with k_{10} = 20 (upper curve) or 30 (lower curve) sec^{-1}; dashed line, prediction of Stein *et al.* model.

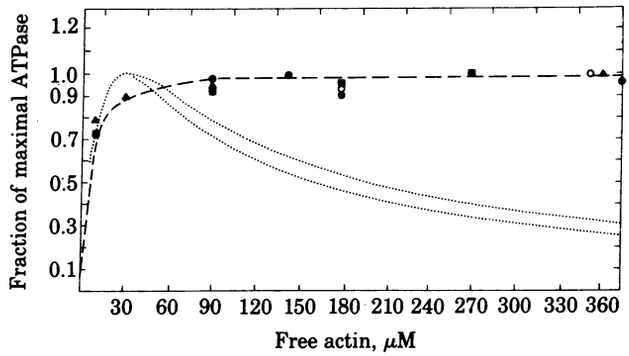

FIG. 5. Actin-activated ATPase activity at high actin concentration. Conditions as in Fig. 1 except 0.2 μM S-1 was used. Different symbols represent different experiments. In each experiment the ATPase activity was normalized to the maximal ATPase activity observed in that particular experiment. These maximal rates varied from 4.0 to 5.0 sec^{-1}. Dotted lines, predictions of Lymn–Taylor model with k_{10} = 20 (upper curve) or 30 (lower curve) sec^{-1}; dashed line, prediction of Stein *et al.* model.

of the initial P_i burst is much greater than is predicted by the Lymn–Taylor model.

Steady-State ATPase Activity. As a final test of the Lymn–Taylor model, we measured the steady-state ATPase rate at very high actin concentration. In previous studies, using the pH-stat to measure ATPase rates, we found no evidence of a decrease in ATPase activity at 200 μM actin (3). In the present study we assayed P_i directly which enabled us to work at an actin concentration as high as 360 μM at which more than 90% of the S-1 is bound to actin in the presence of ATP. Under this condition, the Lymn–Taylor model predicts the ATPase rate should decrease by 70% but, in marked disagreement with this prediction, no decrease in ATPase activity was observed (Fig. 5).

DISCUSSION

We have shown that the rate of the initial P_i burst increases with increasing actin concentration, that at high actin concentration the initial P_i burst has a significant magnitude, and that there is no inhibition of the steady-state ATPase activity at very high actin concentration. All of these observations appear to contradict the predictions of the Lymn–Taylor model in which detachment of actin is mandatory for ATP hydrolysis to proceed. Attempts to fit the observed data to Scheme I have failed because, with the exception of k_{10}, the value of all of the relevant constants have now been determined experimentally. In addition, the value of k_{10} is limited by the steady-state ATPase data (Fig. 1*b*) and by the fact that a high value of k_{10} would yield not only a faster rate for the initial P_i burst but also a decrease in its amplitude. In other words, when the value of k_{10} is chosen to yield a better fit to the fluorescence data in Fig. 3, it yields a poorer fit to the amplitude data in Fig. 4. Therefore, it is not possible to find a k_{10} value that can account for all of the observations in this paper.

The mandatory detachment step in the Lymn–Taylor model was based on the observation that, at low actin concentration, ATP causes dissociation of the acto–heavy meromyosin complex prior to ATP cleavage (1). Our data are consistent with this observation. However, this observation does not show that there is a mandatory detachment step; it only shows that S-1·ATP is in rapid equilibrium with acto–S-1·ATP and that, because the tight binding of ATP greatly reduces the affinity of S-1 for actin, this equilibrium is shifted toward S-1·ATP at low actin concentration. At high actin concentration, where the equilibrium is shifted toward acto–S-1·ATP we now find that the initial P_i burst

occurs at an even faster rate than in the absence of actin. To explain these data a kinetic scheme which does not include a mandatory detachment step is required. Such a model was previously proposed by Stein *et al.* (3):

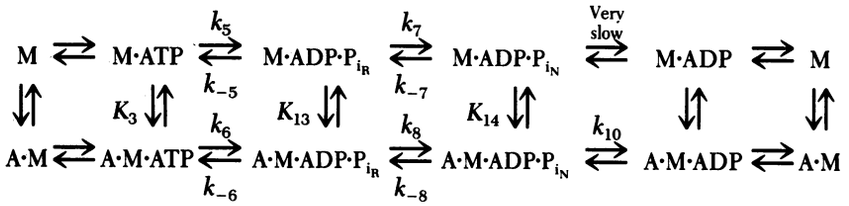

Scheme II

In testing whether this model could explain the data presented in this paper, we made the following assumptions for constants: $k_5 = 17\ sec^{-1}$; $k_{-5} = 6\ sec^{-1}$; $k_6 = 30\ sec^{-1}$; $k_6 = 11\ sec^{-1}$; $k_7 = k_8 = 9\ sec^{-1}$; $k_{-7} = k_{-8} = 45\ sec^{-1}$; $k_{10} = 400\ sec^{-1}$; $K_3 = K_{13} = K_{14} = 3 \times 10^4\ M^{-1}$. The dashed lines in Figs. 1, 3, 4, and 5 show the kinetic behavior predicted by the model of Stein *et al.* with these constants. With the exception of the rate of P_i production (Fig. 4), the predicted curves are in good agreement with the observed data. Because the slow rate observed for P_i production probably can be accounted for by the relatively slow mixing time of viscous solutions in the three-syringe quenched-flow apparatus, the kinetic model of Stein *et al.* seems to provide an adequate explanation for the data.

The fact that the rate of the initial P_i burst is markedly increased at high actin concentration (Fig. 3) suggests that the rate of the P_i burst is even faster when S-1 is bound to actin than when it is dissociated. The finding that the ATP hydrolysis step occurs so rapidly when S-1 is bound to actin takes away the special significance this kinetic step had in the Lymn–Taylor cross-bridge model (1); there is no longer any reason to assume that this step is associated with a change in the preferred angle of attachment of the cross-bridge from 45° back to 90° (1). The data in this paper also rule out the postulate of the original refractory-state model—that the hydrolysis step produces a state that is unable to bind to actin (12, 13). However, the discrepancy observed in Fig. 1 *b* and 4 *a*, showing that the free actin concentration required to obtain half-maximal ATPase activity (5.5 μM) is significantly lower than that required to attain 50% of the S-1 bound to actin (31 μM), can best be explained by postulating a reaction step involving the transition between R and N states (refractory and nonrefractory states) for both the actin-associated and -dissociated S-1·ADP·P_i complex (see scheme II) (3).

The absence of a mandatory detachment step from the actomyosin ATPase cycle *in vitro* has implications for the type of cross-bridge cycle that may occur *in vivo*. Kinetic models with a mandatory detachment step suggested *in vivo* models in which the cross-bridge irreversibly attached to and detached from actin during each cycle of ATP hydrolysis (1, 2). In contrast, the kinetic model of Stein *et al.* (3) suggests that the myosin cross-bridge may not undergo an attachment/detachment cycle each time an ATP molecule is hydrolyzed *in vivo*. Rather, as suggested by Eisenberg and Greene (2), the myosin bridge may cycle between states weakly attached to actin with a preferred angle near 90° (A·M·ATP, A·M·ADP·P_{i_R}, and A·M·ADP·P_{i_N}) and states strongly attached to actin with a preferred angle near 45° (A·M·ADP and A·M). Because there is no mandatory detachment step, the bridge may detach only when, during isotonic contraction, it is elastically distorted and is thus in rapid equilibrium with an unattached state. In the isometric state, the cross-bridge may hydrolyze ATP without cyclically attaching to and detaching from actin; it may simply oscillate between the weakly bound and strongly bound states. Thus, the absence of a mandatory detachment step *in vitro* suggests that cross-bridge detachment *in vivo* may be a mechanical event rather than a strictly biochemical process (2).

We thank Mr. Louis Dobkin for his technical assistance. This work was performed during the tenure of the George Meany Postdoctoral Fellowship awarded by the Muscular Dystrophy Association to L.A.S. This work shall serve as part of the thesis toward the Ph.D. degree in Chemical Physics at the University of Maryland for L.A.S.

1. Lymn, R. W. & Taylor, E. (1971) *Biochemistry* **10**, 4617–4624.
2. Eisenberg, E. & Greene, L. E. (1980) *Annu. Rev. Physiol.* **42**, 293–309.
3. Stein, L. A., Schwarz, R. P., Chock, P. B. & Eisenberg, E. (1979) *Biochemistry* **18**, 3895–3909.
4. Sleep, J. A. & Hutton, R. L. (1978) *Biochemistry* **17**, 5423–5430.
5. Kielley, W. W. & Harrington, W. F. (1960) *Biochim. Biophys. Acta* **41**, 401–421.
6. Eisenberg, E. & Kielley, W. W. (1974) *J. Biol. Chem.* **249**, 4742–4748.
7. Weeds, A. G. & Taylor, R. S. (1975) *Nature (London)* **257**, 54–57.
8. Chock, S. P. & Eisenberg, E. (1979) *J. Biol. Chem.* **254**, 3229–3235.
9. Eisenberg, E. & Moos, C. (1967) *J. Biol. Chem.* **242**, 2945–2951.
10. Johnson, K. A. & Taylor, E. W. (1978) *Biochemistry* **17**, 3432–3442.
11. Chock, S. P., Chock, P. B. & Eisenberg, E. (1979) *J. Biol. Chem.* **254**, 3236–3243.
12. Eisenberg, E. & Kielley, W. W. (1972) *Cold Spring Harbor Symp. Quant. Biol.* **37**, 145–152.
13. Chock, S. P., Chock, P. B. & Eisenberg, E. (1976) *Biochemistry* **15**, 3244–3253.